Journal of Solid State Chemistry **142,** 168–173 (1999)
Article ID jssc.1998.8014, available online at http://www.idealibrary.com on IDEAL®

Synthesis, Structure, and Magnetism of $CN_3H_6 \cdot VO(H_2O)(HPO_4)(H_2PO_4) \cdot H_2O$, a New Guanidinium Vanadium(IV) Phosphate

Zsolt Bircsak,* Annegret K. Hall,† and William T. A. Harrison*,[1]

*Department of Chemistry, and †Special Research Centre for Advanced Mineral and Materials Processing, University of Western Australia, Nedlands, Western Australia 6907, Australia

Received June 1, 1998; in revised form August 17, 1998; accepted August 18, 1998

The solution-phase synthesis, single crystal structure, and some physical properties of $CN_3H_6 \cdot VO(H_2O)(HPO_4)(H_2PO_4) \cdot H_2O$, a new guanidinium vanadium (IV) hydrogen phosphate hydrate, are reported. This phase is built up from one-dimensional chains of $VO_5(H_2O)$ octahedra and $(H_2/H)PO_4$ tetrahedra and fused together via V–O–P linkages. These chains are arranged in "crisscross" configuration from layer to layer. Guanidinium cations and water molecules are arrayed in the interchain regions and link the chains together through a hydrogen bonding network. Magnetic susceptibility data for this phase are also reported. Crystal data: $CN_3H_6 \cdot VO(H_2O)(HPO_4)(H_2PO_4) \cdot H_2O$, $M_r = 356.02$, monoclinic, space group $C2/c$ (No. 15), $a = 13.956(2)$ Å, $b = 11.717(2)$ Å, $c = 13.961(2)$ Å, $\beta = 94.47(1)^\circ$, $V = 2276.1(5)$ Å^3, $Z = 8$, $R = 2.95\%$, $R_w = 3.27\%$ [170 parameters, 2537 observed reflections with $I > 3\sigma(I)$].

INTRODUCTION

An astonishing variety of novel phases arise from the combination of vanadium/phosphate progenitors and small organic molecules (1–8). Such structural variety arises due to the versatility of vanadium in terms of its variable oxidation state (V^{III}, V^{IV}, and V^{V}) and coordination geometry (tetrahedral, square pyramidal, trigonal bipyramidal, and octahedral), combined with the structure-directing (templating) effect of the organic moiety, although, as yet, we have little *control* over such synthesis processes. We have recently reported the synthesis and characterization of $(CN_3H_6)_2 \cdot (VO_2)_3(PO_4)(HPO_4)$, the first guanidinium vanadium(V) phosphate (9). This phase is closely related to the $M(VO_2)_3(SeO_3)_2$ [$M = NH_4$ (10), K (11)] structure, which is based on the hexagonal tungsten oxide (HTO) motif of vertex-sharing VO_6 octahedral layers.

In this paper, we report the synthesis, single-crystal structure, and physical characterization of $CN_3H_6 \cdot VO(H_2O)(HPO_4)(H_2PO_4) \cdot H_2O$, the first guanidinium vanadium (IV) phosphate hydrate. This phase has a crystal structure that is completely different from that of $(CN_3H_6)_2 \cdot (VO_2)_3(PO_4)(HPO_4)$ and shows strong one-dimensional character and structural similarity to known barium vanadium(IV) phosphates in terms of its constituent $[VO(H_2O)(HPO_4)(H_2PO_4)]^-$ chains. In the title compound, these chains adopt a distinctive "crisscross" motif between layers.

EXPERIMENTAL

Synthesis and physical characterization. $CN_3H_6 \cdot VO(H_2O)(HPO_4)(H_2PO_4) \cdot H_2O$ was prepared from a mixture of guanidinium carbonate $[(CN_3H_6)_2CO_3]$ (0.31 g), 85% H_3PO_4 (1.60 g), VCl_3 (0.27 g), V_2O_5 (0.16 g), and 5 ml deionized water (starting molar ratio of guanidine : V : P = 1 : 1 : 4). The components were sealed in a 23-ml capacity Teflon-lined hydrothermal bomb and heated to 120°C for 1 day. The bomb was cooled and opened to result in a blue solution. This was left to crystallize in a petri dish. After 1 month, the solid product, consisting of a homogeneous mass of transparent aqua blue rod-like crystals (0.79 g, 63% yield based on V) of the title compound was recovered from the supernatant liquors by filtration.

Magnetic susceptibility data for a well ground, turquoise sample of $CN_3H_6 \cdot VO(H_2O)(HPO_4)(H_2PO_4) \cdot H_2O$ were collected on a Quantum Design MPMS-7 SQUID magnetometer over the temperature range 5–300 K, using an applied field of 1.2 kG.

Single-crystal structure determination. A crystal of $CN_3H_6 \cdot VO(H_2O)(HPO_4)(H_2PO_4) \cdot H_2O$ (aqua blue rod,

[1]To whom correspondence should be addressed. E-mail: wtah@chem.uwa.edu.au.

0022-4596/99 $30.00

$\sim 0.1 \times 0.1 \times 0.4$ mm) was glued to a thin glass fiber with cyanoacrylate adhesive and mounted on a Siemens P4 automated diffractometer (graphite monochromated Mo$K\alpha$ radiation, $\lambda = 0.71073$ Å). A *C*-centered monoclinic unit cell was established and optimized by the application of peak-search, centering, indexing, and least-squares routines (69 reflections, $11^\circ < 2\theta < 25^\circ$).

Intensity data were collected at room temperature [25 (2)°C] using the $\theta/2\theta$ scan mode to a maximum 2θ of 60° ($-1 \le h \le 19$, $-1 \le k \le 16$, $-19 \le l \le 19$). Intensity standards, remeasured every 100 observations, showed only statistical fluctuations over the course of the data collection. Absorption was monitored by Ψ scans and a correction (min. = 0.56, max. = 0.57) was applied at the data reduction stage. The raw intensities were reduced to F and $\sigma(F)$ values, the normal corrections for Lorentz and polarization effects were made, and the 3928 measured reflections were merged to 3326 unique data ($R_{int} = 0.023$), with 2537 of these considered observed according to the criterion $I > 3\sigma(I)$.

The systematic absences indicated space groups *Cc* or *C*2/*c*, with intensity statistics suggesting the latter. Most of the atom positions in $CN_3H_6 \cdot VO(H_2O)(HPO_4)(H_2PO_4) \cdot H_2O$ were established by direct methods (12) in the centrosymmetric space group *C*2/*c* (No. 15), which was assumed for the remainder of the crystallographic study. The remainder of the nonhydrogen atoms were located from Fourier difference maps, and a Larson-type secondary extinction correction (13) was optimized to improve the fit of strong, low-angle reflections which showed a systematic $F_{obs} < F_{calc}$ trend. Hydrogen atoms associated with the guanidinium cation were located geometrically by assuming planar sp^2 hybridization about each N atom and an N–H bond length of 0.95 Å. Assuming the presence of vanadium(IV) and the guanidinium cation, the charge balancing requirement necessitated the presence of seven additional protons per formula unit. These were all located from Fourier difference maps and correspond to two water molecules and three P–OH vertices. Difference Fourier maps also showed a significant region ($> 2e/$Å^3) of electron density close to the V(1) species. A disordering effect of the vanadium atom over two adjacent positions, subject to the occupancy constraint $occ[V(1)] + occ[V(2)] = 1.00$, was therefore modeled. Final residuals of $R = 2.95\%$ and $R_w = 3.27\%$ [$w_i = 1/\sigma^2(F)$] were obtained for refinements varying positional and anisotropic thermal parameters for all nonhydrogen atoms [U_{iso} for V(2)] and an atom-type isotropic thermal factor for the hydrogen atoms. Refinements neglecting this V atom disorder effect resulted in significantly higher residuals of $R = 4.00\%$ and $R_w = 4.19\%$. All the least-squares refinements and subsidiary calculations were performed with the Oxford CRYSTALS (14) system. Crystallographic data are summarized in Table 1.

TABLE 1
Crystallographic Parameters for $CN_3H_6 \cdot VO(H_2O)(HPO_4)(H_2PO_4) \cdot H_2O$

Empirical formula	$VP_2O_{11}CN_3H_{13}$
Formula weight	356.02
Crystal system	Monoclinic
a (Å)	13.956 (2)
b (Å)	11.717 (2)
c (Å)	13.961 (2)
β (°)	94.47 (1)
V (Å^3)	2276.1 (5)
Z	8
Space group	*C*2/*c* (No. 15)
T (°C)	25 (2)
λ (Mo$K\alpha$) (Å)	0.71073
ρ_{calc} (g/cm^3)	2.078
μ (cm^{-1})	12.1
Total data	3928
Observed data[a]	2537
Parameters	170
min., max, $\Delta\rho$ (e/Å^3)	−0.43, +0.45
$R(F)$[b]	2.95
$R_w(F)$[c]	3.27

[a] $I > 3\sigma(I)$ after data merging to 3326 reflections.
[b] $R = 100 \times \sum||F_o| - |F_c||/\sum|F_o|$.
[c] $R_w = 100 \times [\sum w(|F_o| - |F_c|)^2/\sum w|F_o|^2]^{1/2}$ with $w_i = 1/\sigma^2(F)$.

RESULTS

Crystal structure of $CN_3H_6 \cdot VO(H_2O)(HPO_4)(H_2PO_4) \cdot H_2O$. Atomic positional and thermal parameters are listed in Table 2, and selected geometrical data are presented in Table 3. This material adopts a new crystal structure built up from guanidinium cations and chains of vertex-sharing $VO_5(H_2O)$ octahedra and HPO_4/H_2PO_4 tetrahedra, fused together via V–O–P bonds. A fragment of the structure showing the atom-labeling scheme is shown in Fig 1, and the unit cell packing is illustrated in Fig. 2.

There are 19 independent nonhydrogen atoms in $CN_3H_6 \cdot VO(H_2O)(HPO_4)(H_2PO_4) \cdot H_2O$, all of which occupy general positions. V(1) and V(2) [$d(V \cdots V) \approx 0.53$ Å] represent positional disorder of the vanadium species in a VO_6 octahedron, with the V(1) site dominating in a $\sim 94:6$ ratio. V(1) and its essentially equivalent disordered partner V(2), adopt distorted octahedral coordination. The presence of one short V(1)=O(5) vertex, a long V(1)–O(6) bond *trans* to this short bond, and four V–O bonds of intermediate length is characteristic of the crystallochemical behavior of vanadium(IV) is related structures (8). The long V(1)–O(6) link actually represents a bond between vanadium and a water molecule, as seen earlier in the phases $Ba_2VO(PO_4)_2 \cdot H_2O$ (15) and $Ba_8(VO)_6(PO_4)_2(HPO_4)_{11} \cdot 3H_2O$ (16) which contain similar one-dimensional V/P/O chains. The bond valence sum (BVS), calculated by the Brown formalism (17), of 3.98 for V(1) is commensurate with

TABLE 2
Atomic Coordinates/Thermal Factors[a] for $CN_3H_6 \cdot VO(H_2O)(HPO_4)(H_2PO_4) \cdot H_2O$

Atom	x	y	z	U_{eq}[b]	Occ[c]
V(1)	0.35604(7)	0.08879(9)	0.51063(6)	0.0124	0.938(5)
V(2)	0.3341(9)	0.062(1)	0.5304(9)	0.011(2)	0.062
P(1)	0.56396(4)	0.09666(5)	0.62789(4)	0.0143	
P(2)	0.33025(4)	0.32962(5)	0.62351(4)	0.0164	
O(1)	0.6157(1)	0.0288(1)	0.7148(1)	0.0231	
O(2)	0.5707(1)	0.2239(1)	0.6487(1)	0.0230	
O(3)	0.4584(1)	0.0570(1)	0.6190(1)	0.0178	
O(4)	0.3832(1)	−0.0670(1)	0.4596(1)	0.0173	
O(5)	0.2553(1)	−0.0236(1)	0.6006(1)	0.0258	
O(6)	0.4168(1)	0.1670(2)	0.4429(1)	0.0294	
O(7)	0.3061(1)	0.2081(1)	0.5964(1)	0.0214	
O(8)	0.2309(1)	0.0805(1)	0.4288(1)	0.0202	
O(9)	0.3173(1)	0.3469(2)	0.7331(1)	0.0290	
O(10)	0.4364(1)	0.3606(1)	0.6057(1)	0.0303	
O(11)	0.5734(2)	0.4326(2)	0.1097(2)	0.0549	
C(1)	0.1412(2)	0.7951(2)	0.3601(2)	0.0282	
N(1)	0.0963(2)	0.7036(2)	0.3233(2)	0.0398	
N(2)	0.1755(2)	0.8722(2)	0.3034(2)	0.0463	
N(3)	0.1510(2)	0.8092(3)	0.4530(2)	0.0521	
H(1)	0.5717	0.1480	0.3645	0.083(4)	
H(2)	0.5891	0.1934	0.2556	0.083(4)	
H(3)	0.7072	0.4380	0.3302	0.083(4)	
H(4)	0.6685	0.3622	0.2357	0.083(4)	
H(5)	0.6264	0.2537	0.4942	0.083(4)	
H(6)	0.6829	0.3750	0.4794	0.083(4)	
H(7)	0.1976	0.0058	0.6084	0.083(4)	
H(8)	0.2601	−0.0539	0.6591	0.083(4)	
H(9)	0.5899	0.0408	0.7722	0.083(4)	
H(10)	0.1501	0.1977	0.2259	0.083(4)	
H(11)	0.0244	0.1932	0.3713	0.083(4)	
H(12)	0.5148	−0.4750	0.6137	0.083(4)	
H(13)	0.5484	−0.4052	0.5537	0.083(4)	

[a] Estimated fractional positional uncertainty for the H atoms: ±0.005 in x, y, and z.

[b] $U_{eq}(Å^2) = 1/3[U_1 + U_2 + U_3]$ [$U_{iso}(Å^2)$ for V(2), atom-type $U_{iso}(Å^2)$ for the H atoms].

[c] Fractional site occupancy, if not unity (constraint occ[V(1)] + occ[V(2)] = 1.00 applied.)

TABLE 3
Bond Distances (Å)/Angles(°) for $CN_3H_6 \cdot VO(H_2O)(HPO_4)(H_2PO_4) \cdot H_2O$[a]

V(1)–O(3)	2.033(2)	V(1)–O(4)	2.007(2)
V(1)–O(5)	2.359(2)	V(1)–O(6)	1.607(2)
V(1)–O(7)	2.001(2)	V(1)–O(8)	2.013(2)
P(1)–O(1)	1.577(2)	P(1)–O(2)	1.521(2)
P(1)–O(3)	1.541(2)	P(1)–O(4)	1.515(2)
P(2)–O(7)	1.505(2)	P(2)–O(8)	1.508(2)
P(2)–O(9)	1.568(2)	P(2)–O(10)	1.564(2)
C(1)–N(1)	1.326(3)	C(1)–N(2)	1.316(3)
C(1)–N(3)	1.303(4)		
O(3)–V(1)–O(4)	87.49(7)	O(3)–V(1)–O(5)	85.09(8)
O(4)–V(1)–O(5)	79.53(8)	O(3)–V(1)–O(6)	99.80(9)
O(4)–V(1)–O(6)	100.76(9)	O(5)–V(1)–O(6)	175.10(8)
O(3)–V(1)–O(7)	86.57(7)	O(4)–V(1)–O(7)	158.8(1)
O(5)–V(1)–O(7)	79.71(8)	O(6)–V(1)–O(7)	100.3(1)
O(3)–V(1)–O(8)	160.4(1)	O(4)–V(1)–O(8)	86.22(7)
O(5)–V(1)–O(8)	75.47(8)	O(6)–V(1)–O(8)	99.66(9)
O(7)–V(1)–O(8)	92.65(7)	O(1)–P(1)–O(2)	109.21(9)
O(1)–P(1)–O(3)	106.69(9)	O(2)–P(1)–O(3)	110.85(9)
O(1)–P(1)–O(4)	106.41(9)	O(2)–P(1)–O(4)	110.6(1)
O(3)–P(1)–O(4)	112.84(9)	O(7)–P(2)–O(8)	115.6(1)
O(7)–P(2)–O(9)	109.1(1)	O(8)–P(2)–O(9)	106.13(9)
O(7)–P(2)–O(10)	112.1(1)	O(8)–P(2)–O(10)	105.6(1)
O(9)–P(2)–O(10)	108.0(1)	V(1)–O(3)–P(1)	128.1(1)
V(1)–O(4)–P(1)	127.7(1)	V(1)–O(7)–P(2)	136.9(1)
V(1)–O(8)–P(2)	132.4(1)	N(1)–C(1)–N(2)	120.4(3)
N(1)–C(1)–N(3)	119.9(3)	N(2)–C(1)–N(3)	119.8(3)

[a] Duplicate and apparent contacts arising due to V(2) omitted.

the expected value of 4.00 for pure vanadium(IV) character. The two distinct HPO_4/H_2PO_4 groups display typical tetrahedral geometry with d_{av}[P(1)–O] = 1.538 Å, BVS[P(1)] = 4.96, d_{av}[P(2)–O] = 1.536 Å, and BVS[P(2)] = 4.99. Both of the these groups form two P–O–V bonds and two terminal P–O linkages (μ-O,O coordination). The P(1)-centered moiety is an HPO_4 group, the P(2)-centered moiety is an H_2PO_4 group. The guanidinium cation shows three essentially equivalent C–N bond lengths [average = 1.315 Å], as seen in other structures templated by this cation (18). There is an extrachain water molecule of crystallization, O(11).

The structural motif in $CN_3H_6 \cdot VO(H_2O)(HPO_4)(H_2PO_4) \cdot H_2O$ consists of infinite chains of $VO_5(H_2O)$ and HPO_4/H_2PO_4 groups, fused together through V–O–P bonds (Fig. 3). Polyhedral "four-rings" result, with strict alternation of the V and P species. The HPO_4 and H_2PO_4 species segregate into their own four-rings. Based on the majority V(1) configuration, the short V(1)=O(6) bonds project from alternate sides of the chain in an ordered fashion (Fig. 3). It is not clear why the partial disorder of V(1) and V(2) occurs. There appears to be no particular advantage in terms of hydrogen bonding interactions involving the majority O(6)=V(1)–O(5)H_2 versus those seen with the minority H_2O(6)–V(2)=O(5) conformation. Both O(5) and O(6) have several neighboring O atoms with d(O···O) ~ 2.8 Å which could act as H-bond acceptors. Each $VO_5(H_2O)$ group forms four V–O–P links ($\theta_{av} = 131.3°$). Unlike the layered guanidinium vanadium(V) phosphate, $(CN_3H_6)_2 \cdot (VO_2)_3(PO_4)(HPO_4)$ (9), there are no V–O–V links in this structure. The resulting chain stoichiometry in the title compound is $[VO(H_2O)(HPO_4)(H_2PO_4)]^-$, with charge compensation provided by a protonated guanidinium cation. The $[VO(H_2O)(HPO_4)(H_2PO_4)]^-$ chains adopt a distinctive arrangement in the unit cell, with alternating layers of chains propagating along [1 1 0] ad [1 $\bar{1}$ 0], with the chain stacking occurring along the c direction (Fig. 2).

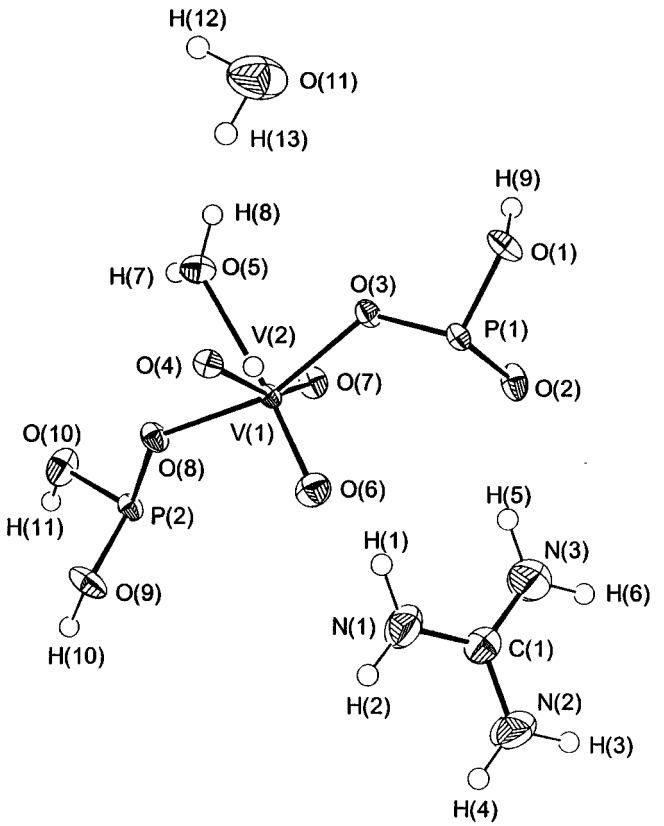

FIG. 1. View of the asymmetric unit of $CN_3H_6 \cdot VO(H_2O)(HPO_4)(H_2PO_4) \cdot H_2O$ showing the atom-labeling scheme (50% thermal ellipsoids; disordered atom V(2) and protons represented by spheres of arbitrary radius).

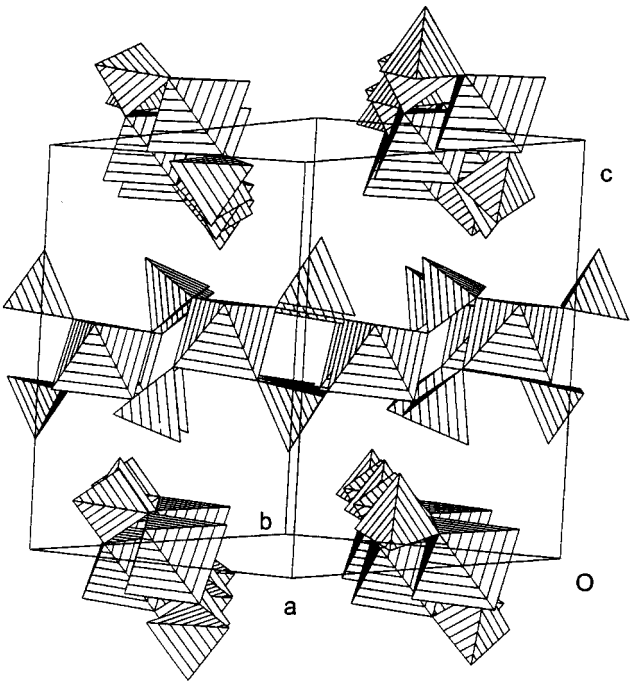

FIG. 2. Polyhedral view approximately down $[1\bar{1}0]$ of the crystal structure of $CN_3H_6 \cdot VO(H_2O)(HPO_4)(H_2PO_4) \cdot H_2O$ showing the criss-cross configuration of the $VO(H_2O)(HPO_4)(H_2PO_4)$ chains built up from $VO_5(H_2O)$ octahedra and $(H/H_2)PO_4$ tetrahedra.

Hydrogen bonding (Table 4) appears to be significant in establishing this crystal structure. An intrachain linkage involves an O(10)–H(11)···O(2) bond. The interchain, *intra*layer connectivity involves both the water molecules and also occurs via the guanidinium cation. The water-molecule linkage involves an O(5)–H(7)···O(11)–H(12)···O(10) bridge, where O(5) is the water molecule attached V(1) and O(11) is the extrachain water molecule. Four of the H atoms associated with the guanidinium cation partake in H bonds, assuming a maximum H-bonding constant distance of 2.3 Å (Fig. 4). Finally, interchain, *inter*layer H bonding is accomplished via O(1)–H(9)···O(3) and O(9)–H(10)···O(2) linkages.

Physical data. Magnetic susceptibility data for $CN_3H_6 \cdot VO(H_2O)(HPO_4)(H_2PO_4) \cdot H_2O$ (Fig. 5) show paramagnetic behavior between 5 and 300 K, with no evidence for any cooperative magnetic phenomena. The higher temperature ($T > 150$ K) data were modeled by a Curie–Weiss type law $[\chi = \chi_0 + C/(T - \theta)]$ (16), resulting in an effective magnetic moment per vanadium atom, μ_{eff}, of 1.81 μ_B, in good agreement with the spin-only value of 1.73 μ_B expected for a d^1 vanadium(IV) containing system (19). The Weiss constant, θ, of -13.3 K, suggests that antiferromagnetic order might occur at very low temperatures, possibly mediated by V–O–P–O–V superexchange interactions.

DISCUSSION

Single crystals of a new guanidinium vanadium(IV) phosphate hydrate, $CN_3H_6 \cdot VO(H_2O)(HPO_4)(H_2PO_4) \cdot H_2O$,

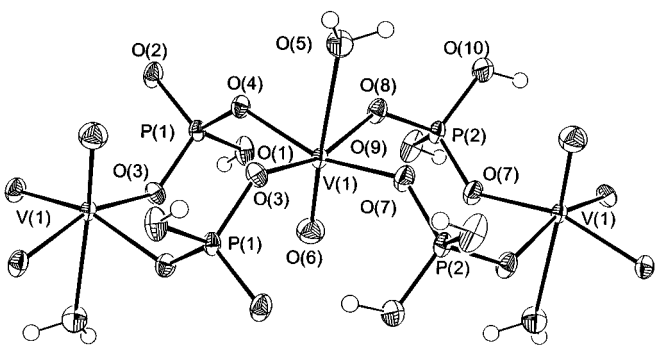

FIG. 3. Fragment of the $CN_3H_6 \cdot VO(H_2O)(HPO_4)(H_2PO_4) \cdot H_2O$ structure showing the $[VO(H_2O)(HPO_4)(H_2PO_4)]^-$ chain, built up from 4-ring polyhedral units. Note that the $HP(1)O_4$ and $H_2P(2)O_4$ groups segregate into their own 4-rings.

TABLE 4
Hydrogen Bonding Distances[a] (Å) for $CN_3H_6 \cdot VO(H_2O)(HPO_4)(H_2PO_4) \cdot H_2O$[a]

N(2)–H(3) ··· O(8)	0.95	2.17	3.067(3)
N(2)–H(4) ··· O(11)	0.95	2.28	3.040(4)
N(3)–H(5) ··· O(4)	0.95	2.29	3.140(4)
N(3)–H(6) ··· O(5)	0.95	2.24	3.121(4)
O(5)–H(7) ··· O(11)	0.89	1.88	2.766(3)
O(5)–H(8) ··· O(9)	0.89	2.24	3.014(3)
O(1)–H(9) ··· O(3)	0.92	1.72	2.633(2)
O(9)–H(10) ··· O(2)	0.88	1.75	2.615(2)
O(10)–H(11) ··· O(2)	0.88	1.65	2.503(2)
O(11)–H(12) ··· O(10)	0.96	2.21	3.805(3)
O(11)–H(13) ··· O(10)	0.89	2.31	3.116(3)

[a] The three distances refer to the X–H, H ··· Y, and X ··· Y separations, respectively, for a X–H ··· Y hydrogen bond. Estimated esds for the O–H, N–H, and H ··· O distances ≈0.05 Å, taking account of the riding scheme used to refine the H atom positions.

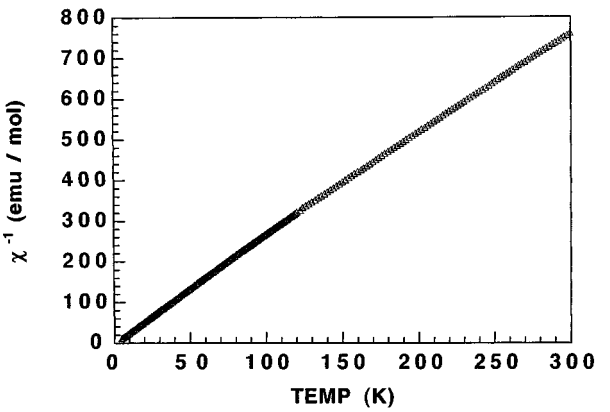

FIG. 5. Plot of inverse molar susceptibility versus temperature for $CN_3H_6 \cdot VO(H_2O)(HPO_4)(H_2PO_4) \cdot H_2O$.

have been prepared from solution and structurally and physically characterized. Pure vanadium(IV) character is well defined in this phase on the basis of BVS calculations, magnetic susceptibility data, $VO_5(H_2O)$ geometry, crystal color, and a reasonable charge balancing scheme.

Structurally, $CN_3H_6 \cdot VO(H_2O)(HPO_4)(H_2PO_4) \cdot H_2O$ has strong one-dimensional character in terms of its "inorganic" V/P/O/H component. The polyhedral chain-linkage pattern of vertex-linked $VO_5(H_2O)/PO_4$ 4-rings is identical to that found in $Ba_2VO(PO_4)_2 \cdot H_2O$ (15), which also shows a disordering effect of the octahedral O=V–OH_2 and H_2O–V=O bonds, although the disordering of the V atom positions is in a crystal-symmetry imposed 50 : 50 ratio in the barium compound. The relative configurations of the VPO chains is quite different in these two phases: Monoclinic $Ba_2VO(PO_4)_2 \cdot H_2O$ shows simple one-dimensional alignment of all the chains along [0 1 0], whereas in $CN_3H_6 \cdot VO(H_2O)(HPO_4)(H_2PO_4) \cdot H_2O$, the crisscross stacking in the c direction results. The unusual vanadium(IV) hypophosphite $VO(H_2PO_2)_2 \cdot H_2O$ (20) shares the 4-ring chain topology (built up from $VO_5(H_2O) + PO_2H_2$ units) with $CN_3H_6 \cdot VO(H_2O)(HPO_4)(H_2PO_4) \cdot H_2O$ and includes a V–OH_2 bond *trans* to the V=O linkage.

An interesting variation on the octahedral/tetrahedral chain topology in the title compound occurs in the recently reported (21) $(HN_3(CH_2)_2NH_3)_{1/2} \cdot VO(H_2O)As_2O_7$ [$VO_5(H_2O)$ octahedra and As_2O_7 bi-tetrahedra], with the As–O–As pyroarsenate link occurring *across* the octahedral/tetrahedral 4-ring. In a broader structural context, Wells (22) has suggested that the prototype compound for the one-dimensional octahedral/tetrahedral 4-ring chain is $K_2Mo_3O_{10}$ [or $K_2(MoO_2)(MoO_4)_2$] (23). The motif of one-dimensional chains of 4-rings also occurs in several phases built up from all-tetrahedral subunits including $NH_4 \cdot H_3N(CH_2)_2NH_3 \cdot Al(PO_4)_2$ (24), $RbZn(HPO_4)(H_2PO_4) \cdot H_2O$ (25), and $HN_3(CH_2)_4NH_3 \cdot Ga(PO_4)(HPO_4)$ (26) [building blocks of $AlO_4 + PO_4$, $ZnO_4 + (H/H_2)PO_4$, and $GaO_4 + (H)PO_4$ tetrahedra, respectively].

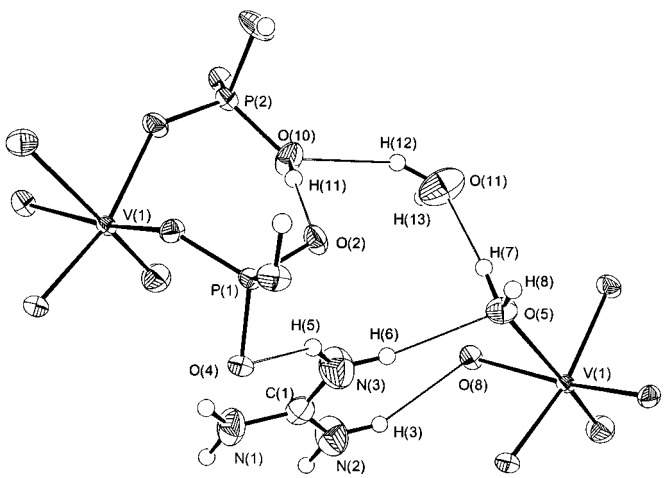

FIG. 4. Detail of the $CN_3H_6 \cdot VO(H_2O)(HPO_4)(H_2PO_4) \cdot H_2O$ structure showing the H bonds (thin lines) involving the guanidinium cation and O(11). The guanidinium cation serves to link adjacent VPO chains in the same layer (see text).

ACKNOWLEDGMENT

We thank the Australian Research Council for financial support.

REFERENCES

1. V. Soghomonian, Q. Chen, R. C. Haushalter, J. Zubieta, and C. J. O'Connor, *Science* **259,** 1596 (1993).
2. V. Soghomonian, Q. Chen, R. C. Haushalter, and J. Zubieta, *Angew. Chem. Int. Ed. Engl.* **32,** 610 (1993).

3. V. Soghomonian, Q. Chen, R. C. Haushalter, and J. Zubieta, *Chem. Mater*. **5,** 1690 (1993).
4. V. Soghomonian, R. C. Haushalter, Q. Chen, and J. Zubieta, *Inorg. Chem.* **33,** 1700 (1994).
5. M. L. Khan, L. M. Meyer, R. C. Haushalter, A. L. Schweizer, J. Zubieta, and J. L. Dye, *Chem. Mater*. **8,** 43 (1996).
6. G. Bonavia, R. C. Haushalter, C. J. O'Connor, and J. Zubieta, *Inorg. Chem.* **35,** 5603 (1996).
7. T. Loiseau and G. Férey, J. *Solid State Chem.* **111,** 416 (1994).
8. W. T. A. Harrison, K. Hsu, and A. J. Jacobson, *Chem. Mater*. **7,** 2004 (1995).
9. Z. Bircask and W. T. A. Harrison, *Inorg. Chem.* **37,** 3204 (1998).
10. J. T. Vaughey, W. T. A. Harrison, L. L. Dussack, and A. J. Jacobson, *Inorg. Chem.* **33,** 4370 (1994).
11. W. T. A. Harrison, L. L. Dussack, and A. J. Jacobson, *Acta Crystallogr. C* **51,** 2473 (1995).
12. G. M. Sheldrick, SHELXS86 User Guide, University of Göttingen, Germany (1986).
13. A. C. Larson, *Acta Crystallogr.* **23,** 664 (1967).
14. D. J. Watkin, J. R. Carruthers, and P. W. Betteridge, CRYSTALS User Guide, Chemical Crystallogrphy Laboratory, Univ. of Oxford, UK.
15. W. T. A. Harrison, S. C. Lim, J. T. Vaughey, A. J. Jacobson, D. P. Goshorn, and J. W. Johnson, *J. Solid State Chem.* **113,** 444 (1994).
16. W. T. A. Harrison, J. T. Vaughey, A. J. Jacobson, D. P. Goshorn, and J. W. Johnson, *J. Solid State Chem.* **116,** 77 (1995).
17. I. D. Brown, *J. Appl. Crystallogr.* **29,** 479 (1996).
18. W. T. A. Harrison and M. L. F. Phillips, *Chem. Mater*. **9,** 1837 (1997).
19. R. L. Carlin, "Magnetochemistry," Springer-Verlag, New York, 1986.
20. A. Le Bail, M. D. Marcos, and P. Amorós, *Inorg. Chem.* **33,** 2607 (1994).
21. A.-H. Liu and S.-L. Wang, *Inorg. Chem.* **37,** 3415 (1998).
22. A. F. Wells, "Structural Inorganic Chemistry," 5th ed., p. 236. Oxford Science Publications, New York, 1984.
23. B. M. Gatehouse and P. Leverett, *J. Chem. Soc*. 1398 (1968).
24. Q. Gao, J. Chen, S. Li, R. Xu, J. M. Thomas, M. Light, and M. B. Hursthouse, *J. Solid State Chem.* **127,** 145 (1996).
25. W. T. A. Harrison, Z. Bircsak, and L. Hannooman, *J. Solid State Chem.* **134,** 148 (1997).
26. A. M. Chippindale, A. D. Bond, A. D. Law, and A. R. Cowley, *J. Solid State Chem.* **136,** 227 (1998).